Neuron, Vol. 28, 411–425, November, 2000, Copyright ©2000 by Cell Press

Mesenchymal/Epithelial Induction Mediates Olfactory Pathway Formation

Anthony-Samuel LaMantia,*‡ Naina Bhasin,* Kattron Rhodes,* and Jill Heemskerk†
*Department of Cell and Molecular Physiology and Center for Neuroscience
The University of North Carolina at Chapel Hill, Medical School
Chapel Hill, North Carolina 27599
†National Institute for Neurological Diseases and Stroke
Betheseda, Maryland 20892

Summary

In the olfactory pathway, as in the limbs, branchial arches, and heart, mesenchymal/epithelial induction, mediated by retinoic acid (RA), FGF8, sonic hedgehog (*shh*), and the BMPs, defines patterning, morphogenesis, and differentiation. Neuronal differentiation in the olfactory epithelium and directed growth of axons in the nascent olfactory nerve depend critically upon this inductive interaction. When RA, FGF8, *shh*, or BMP signaling is disrupted, distinct aspects of olfactory pathway patterning and differentiation are compromised. Thus, a cellular and molecular mechanism that facilitates musculoskeletal and vascular development elsewhere in the embryo has been adapted to guide the differentiation of the olfactory pathway in the developing forebrain.

Introduction

From the earliest descriptions of neural development, a mystery has confronted embryologists—are there tissue–tissue interactions that induce the differentiation of forebrain regions and pathways? Unlike the spinal cord and hindbrain where signals from the notochord, somites, and dorsal ectoderm influence differentiation (reviewed by Tanabe and Jessell, 1996), there is no known source of inductive signals for specific forebrain subdivisions or related neural structures (reviewed by Lumsden and Krumlauf, 1996; Rubenstein and Beachy, 1998). At several embryonic sites outside the central nervous system, including the limbs, branchial arches, and heart, induction between mesenchyme and adjacent epithelia underlies local axis formation, morphogenesis, and differentiation (reviewed by Tickle and Eichele, 1994; Johnson and Tabin, 1997; Creazzo et al., 1998). We asked whether a similar inductive mechanism between the mesenchyme of the frontonasal mass and adjacent epithelia mediates differentiation of a major component of the forebrain—the olfactory pathway.

As in the limbs, branchial arches, and heart, the surface epithelium of the head, the frontonasal mesenchyme, and the forebrain neuroepithelium are apposed to one another and thus are well positioned to exchange inductive signals. These embryonic primordia undergo changes consistent with mesenchymal/epithelial induction. The surface epithelium thickens and invaginates to form the olfactory pit (Jacobson, 1963; Cuschieri and Bannister, 1975), the ventrolateral telencephalon thickens and invaginates to form the olfactory bulb (Hinds, 1968), and the mesenchyme condenses to form cartilage and bone in the nose (Richman and Tickle, 1989). In addition, as is the case for the mesenchyme of the limbs, heart, and branchial arches (Le Lievre and Le Dourain, 1975; Rollhauser-ter Horst, 1975; Lumsden, 1988; Waldo et al., 1996), neural crest contributes to the frontonasal mesenchyme (Serbedzija et al., 1992; Osumi-Yamashita et al., 1994). Finally, there are several inductive signaling molecules present in epithelia or mesenchyme of the olfactory primordia. These include retinoic acid (RA), fibroblast growth factor 8 (*FGF8*), sonic hedgehog (*shh*), and bone morphogenetic protein 4 *(BMP4*; Echelard et al., 1993; LaMantia et al., 1993; Francis-West et al., 1994; Heikinheimo et al., 1994; Crossley and Martin, 1995). While it is generally agreed that none of these factors act alone to mediate induction and differentiation (for review see Johnson and Tabin, 1997), their availability suggests that molecular signaling between epithelium and mesenchyme can influence early olfactory pathway development.

Despite these suggestions, there is no evidence that mesenchymal/epithelial induction contributes to olfactory pathway development. In fact, there is still controversy over whether formation of the olfactory epithelium and nerve relies upon cell migration from the neural tube and long distance signals from the forebrain versus local signals between epithelium and mesenchyme (reviewed by Farbman, 1988, 1992). We therefore asked if there is mesenchymal/epithelial induction in the nascent olfactory pathway. We found that induction mediated by local molecular signals orchestrates axis formation, patterned gene expression, morphogenesis, and cellular differentiation during the initial formation of the olfactory epithelium and nerve.

Results

Mesenchymal/Epithelial Apposition in the Frontonasal Mass and Forebrain

We first defined the relationship between mesenchyme and epithelium in the primordial olfactory pathway. As early as E8.0, there are distinct mesenchymal and epithelial compartments in the frontonasal region (Figure 1A). A coherent mass of mesenchymal cells separates the surface epithelium of the head (which gives rise to the olfactory epithelium) and the forebrain neuroepithelium (which gives rise to the olfactory bulb). A subpopulation of neural crest–associated cells in the frontonasal mesenchyme can be visualized using a gene-trap mouse (the β*geo*6 mouse) where β-galactosidase (β-gal) labels cells in all targets of cranial neural crest including the frontonasal region (Figures 1A and 1B). These cells can be specifically double labeled by antibodies against nes-

‡To whom correspondence should be addressed (e-mail: anthony_lamantia@med.unc.edu).

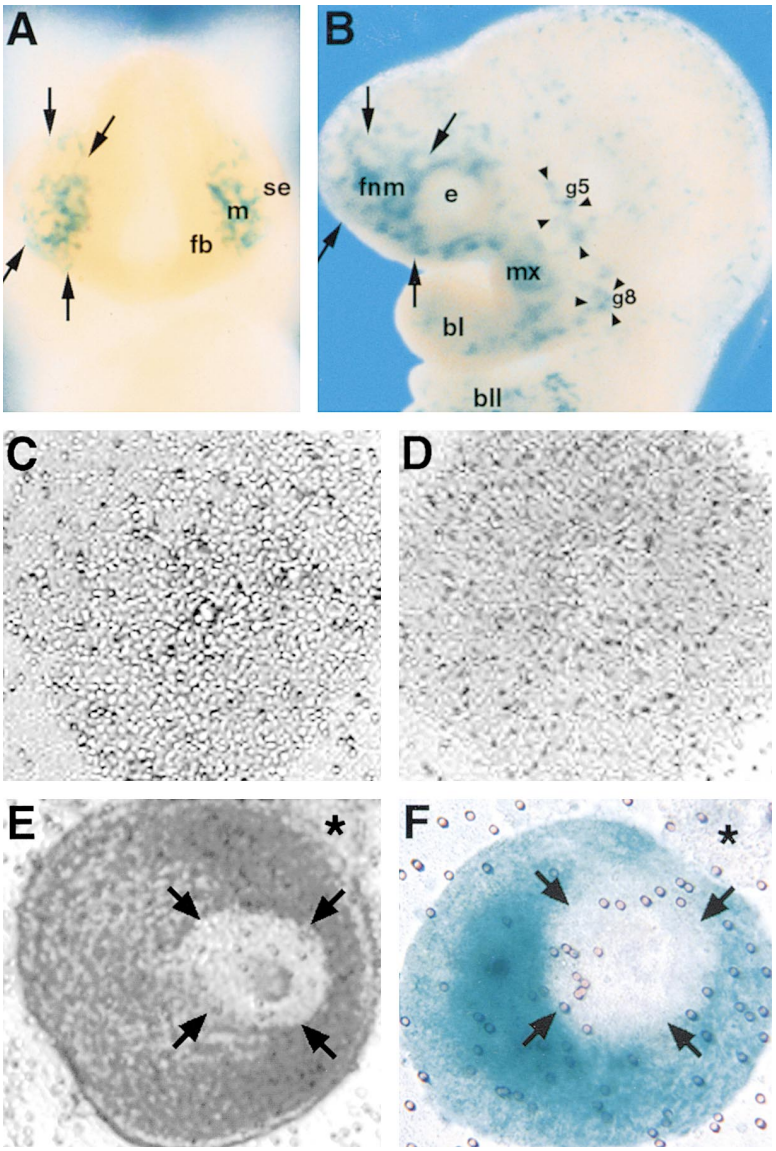

Figure 1. Mesenchymal/Epithelial Apposition in the Developing Olfactory Pathway

(A) Front view of an E8.5 β*geo*6 embryo showing β-galactosidase-labeled cells in the frontonasal mesenchyme (m) between the forebrain (fb) and the lateral surface epithelium of the head (se).

(B) At E 9.0 the β*geo*6 locus is expressed in the rudimentary fifth and eight cranial ganglia (g5 and g8), as well as mesenchyme in the first and second branchial arch (bI and bII), maxillary process (mx), around the eye (e), and frontonasal mass (arrows, fnm).

(C) Live image of an E9.0 isolated surface epithelium showing no differentiation after 48 hr in culture.

(D) Live image of E9.0 frontonasal mesenchyme showing no differentiation after 48 hr in culture.

(E) Live image of an explant where surface epithelium and mesenchyme have been recombined. After 48 hr in culture, an epithelial region thickens and invaginates (arrows). There is also a single, distinct spherical mass of cells at the periphery of the explant (asterisk).

(F) ROSA26 mesenchyme recombined with wild-type epithelium. The mesenchyme is labeled by β-gal, reflecting its ROSA26 origin, while the presumed olfactory pit (arrows) and peripheral cell mass (asterisk) is unlabeled, indicating that these cells come from the wild-type epithelium.

tin, an established marker for neural crest in mammals (Stemple and Anderson, 1992; data not shown), and GAP43, also seen in crest derivatives (Benowitz et al., 1988; data not shown). Thus, a molecularly distinct population of neural crest–associated mesenchymal cells is immediately adjacent to cranial epithelia that give rise to the olfactory pathway.

Mesenchymal/Epithelial Interactions and Morphogenesis

To determine if inductive interactions occur between the frontonasal mesenchyme and epithelia, we cultured undifferentiated surface epithelium and mesenchyme from the frontonasal mass of E9.0 embryos separately or recombined. We first assessed the morphogenetic capacity of isolated or recombined tissues after 48 hr in culture. Isolated epithelium remains a single-cell layer and shows little cytological differentiation (Figure 1C). Frontonasal mesenchyme also remains an undifferentiated cell mass (Figure 1D). In contrast, when the two are recombined, a distinct subregion of the epithelium thickens, invaginates, and resembles the olfactory pit in intact E10.5/E11 embryos (Figure 1E; Table 1). In addition, there is a single spherical mass of cells at the periphery of the explant (Figure 1E, asterisk).

We then assessed whether morphogenesis depends upon cell–cell signaling versus cell migration between mesenchyme and epithelia. We recombined wild-type epithelium with mesenchyme from ROSA26 embryos in which every cell is labeled by β-gal (Zambrowicz et al., 1997). After 48 hr, the thickened epithelium consists of wild-type cells (i.e., unlabeled by β-gal; Figure 1F), while the mesenchyme consists of ROSA26 cells. There is no detectable migration of mesenchymal cells into the pit-like structure. There is, however, an apparent translocation of epithelial cells through the mesenchyme. These cells are seen in the peripheral cell mass at the explant perimeter (Figure 1F, asterisk). Accordingly, apposition of the frontonasal mesenchyme and surface epithelium leads to local epithelial differentiation and subsequent

Table 1. Morphological Differentiation of Epithelial, Mesenchymal, and Recombined Cultures

	Result			
Type of Culture	Differentiated (+)	Undifferentiated (−)	+/−	Percent +
Surface Epithelium	0	33	7	17.5%
Mesenchyme	0	16	3	15%
Recombined	29	2	6	78%

Morphological differentiation was assessed in 96 cultures from 9 litters of E9.0 embryos. After 48 hours in vitro, live images were evaluated. To be scored as differentiated, the culture had to show a thickened and invaginated epithelial pit, a complete covering of epithelium, and underlying mesenchymal mass. To be scored as undifferentiated, surface epithelial cultures had to show a single-cell-thick epithelial sheet, and mesenchymal cultures had to show a coherent, undifferentiated cell mass. The +/− category included recombined cultures where the presumptive olfactory epithelium had not completely invaginated or the mesenchyme was not completely covered by an overlying epithelium. Surface epithelial cultures with small patches of thickened epithelial cells were assigned to this category, as were mesenchymal cultures with any indication of nonuniform cell groups in the mesenchymal mass.

formation of an olfactory pit-like structure. This morphogenesis must depend upon molecular signaling between mesenchyme and epithelium since there is no indication that cells migrate between the two tissue compartments.

Mesenchymal/Epithelial Induction, Cellular and Molecular Differentiation in the Olfactory Pathway

We next asked whether mesenchymal/epithelial induction in the olfactory primordia influences patterned expression of molecules associated with differentiation in the olfactory pathway. The neuroblast marker β-tubulin distinguishes the olfactory epithelium at midgestation (Easter et al., 1993; Whitesides and LaMantia, 1996; Roskams et al., 1998). β-tubulin cannot be detected in the frontonasal region of E9.0 embryos from which epithelium and mesenchyme are cultured (Figure 2, first column). Subsequently, at E10, β-tubulin is expressed in a patch of surface epithelial cells. As the olfactory pit invaginates, β-tubulin defines the entire presumptive olfactory epithelium as well as the nascent olfactory nerve. In recombined cultures, β-tubulin is expressed in the epithelial pit and the peripheral cell mass. β-tubulin is not seen when the epithelium is cultured alone and is occasionally expressed in scattered cells in the isolated mesenchyme.

The retinoid synthesizing enzyme retinaldehyde dehydrogenase 2 (RALDH2) contributes to RA synthesis in the developing nervous system (Zhao et al., 1996; Sockanathan and Jessell, 1998; Niederrethier et al., 1999), perhaps including the frontonasal region where RA is locally available (LaMantia et al., 1993). RALDH2 is not expressed in the frontonasal mass at E9.0, although it is present in the optic vesicle (Figure 2, second column). Subsequently, RALDH2 is seen in the lateral–posterior frontonasal process. A similar pattern is seen in recombined epithelium and mesenchyme. RALDH2 is not expressed in isolated epithelium; in contrast, it persists in a central mass of isolated mesenchymal cells.

The neural cell adhesion molecule (NCAM) is diagnostic for differentiating olfactory epithelial neurons in vivo and in vitro (Calof and Chikaraishi, 1989; Croucher and Tickle, 1989; Miragall et al., 1989; Key and Akeson, 1990; Schwanzel-Fukuda et al., 1992; Whitesides and LaMantia, 1996; Shou et al., 1999). NCAM is not expressed in olfactory primordia at E9.0 (Figure 2, third column) but delineates the epithelium and nerve by E11. In recombined cultures, NCAM is seen in cells concentrated in an epithelial subregion as well as in neurites that form bundles and coalesce into an apparent nerve in the mesenchyme. In addition, NCAM labels the peripheral cell mass. These cells may be either the precursors of GNRH neurons that migrate from the olfactory epithelium along the olfactory nerve toward the brain (Wray et al., 1989; Schwanzel-Fukuda et al., 1992) or precursors of ensheathing cells that will provide glial investment for mature olfactory axons (Doucette, 1990). NCAM is not seen in isolated epithelium or mesenchyme.

The transcription factor Pax-7 is expressed primarily in the mesenchyme of the lateral nasal process, and when this gene is inactivated, some lateral nasal structures do not develop (Mansouri et al., 1996). Pax-7 is not detected in olfactory primordia at E9.0 (Figure 2, fourth column). At E10, however, prior to morphogenesis of the lateral nasal process, Pax-7 is seen in the lateral frontonasal mesenchyme. By E11, Pax-7 clearly distinguishes the lateral from the medial mesenchyme. In recombined cultures, Pax-7 is limited to mesenchyme on one side of the apparent olfactory epithelium but is not seen in the peripheral cell mass. Pax-7 is not detected in isolated epithelium or mesenchyme.

Finally, we asked whether apparent regional distinctions in neural and mesenchymal markers reflect axes that constrain olfactory pathway assembly. In the embryo, Pax-7 defines a medial–lateral boundary that extends the entire anterior–posterior length of the frontonasal mesenchyme (Figures 3A and 3C). Pax-7 is also seen in epithelial cells at the lateral margin of the nasal pit (Figure 3E, arrowheads). NCAM-labeled cells are limited to the medial aspect of the invaginated olfactory epithelium (Figures 3B, 3D, and 3E), and NCAM-labeled axons follow the medial–lateral boundary defined by Pax-7 expression (Figure 3E); however, they extend only toward the anterior pole of the forebrain (Figure 3D). These medial–lateral and anterior–posterior distinctions are maintained in vitro (Figure 3F).

Local Sources of Signaling Molecules in the Developing Olfactory Pathway

We next explored whether specific molecular signals from either the mesenchyme or epithelium are locally available to contribute to induction, axis formation, and subsequent differentiation. We focused upon four signals—RA, *FGF8*, *shh*, and *BMP4*—each of which is

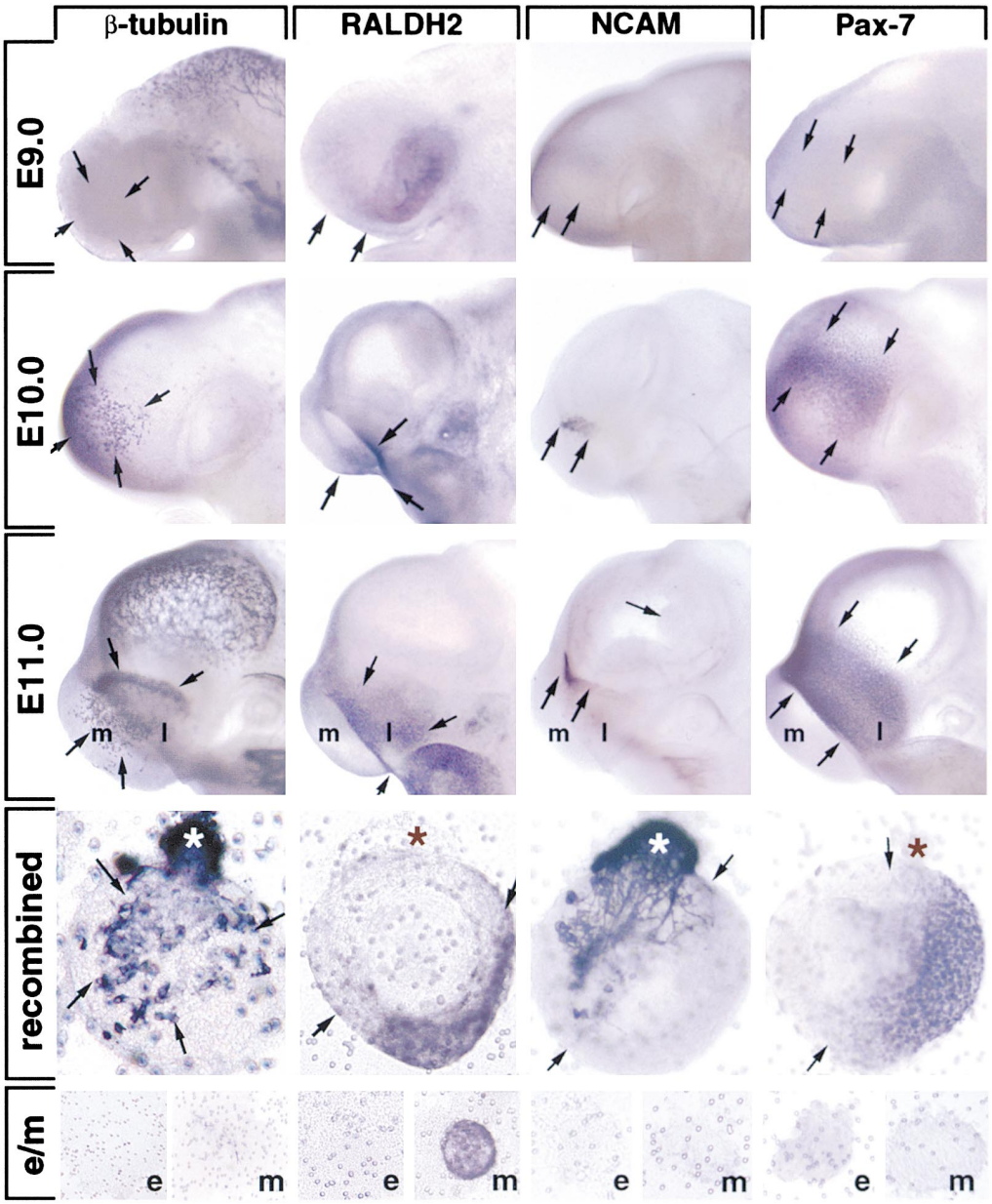

Figure 2. Patterning and Differentiation in the Olfactory Pathway Depends upon Mesenchymal/Epithelial Apposition

In each column, labeling for a marker associated with cellular differentiation in the olfactory pathway is shown. Arrows in each panel indicate either the olfactory primordia or the region within the olfactory primordia where the relevant molecule is expressed. The first three panels of each column show the chronology and pattern of expression of each marker in embryos between E9.0 and E11.0—the times when cultures are initiated and terminated. The last two panels of each column show the expression and pattern of these markers in recombined epithelial/mesenchymal cultures, isolated epithelium, and mesenchyme (e or m, as indicated at bottom right of each panel).

thought to contribute to patterning and morphogenesis in limbs (reviewed by Johnson and Tabin, 1997), branchial arches (Helms et al., 1997; Francis-West et al., 1998), and heart (Laufer et al., 1994; Vogel et al., 1996).

We have previously established that the frontonasal mesenchyme provides a local source of RA for the developing forebrain (LaMantia et al., 1993). The location of neural crest–associated mesenchyme in the lateral frontonasal mass is in register with domains of RA-mediated gene expression in the olfactory epithelium and forebrain (Figures 4A and 4B). To evaluate whether the position of crest cells is related to the local source of RA, we cultured the frontonasal mass from E10.0 β*geo*6 embryos, mesenchyme side down, on monolayers of an RA indicator cell line (LaMantia et al., 1993) reengineered with green fluorescent protein (GFP) as the reporter. In these cocultures, we saw RA-activated GFP-expressing indicator cells (in the monolayer underlying the explant) only beneath β*geo*6-expressing mesenchymal cells in the lateral aspect of the explant (Figures 4C and 4D). We confirmed this using mutant *Pax-6*^{Sey}/*Pax-6*^{Sey} (*small*

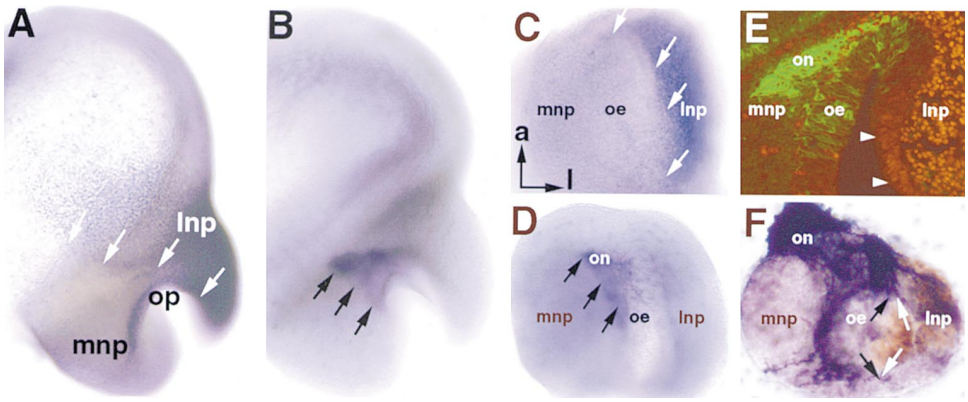

Figure 3. Medial–Lateral and Anterior–Posterior Axes in the Developing Olfactory Pathway Depend upon Mesenchymal/Epithelial Inductive Signaling

(A) Front view of an E10.5 embryo forebrain and frontonasal mass immunolabeled for Pax-7, showing the unlabeled medial nasal process (mnp), the labeled lateral nasal process (lnp), and the olfactory pit (op) between the two. The white arrows indicate the border between the Pax-7-labeled lateral and the unlabeled medial mesenchyme.

(B) Front view of an E10.5 embryo shows NCAM-labeled cells and axons in the olfactory epithelium and nerve. The black arrows indicate NCAM-positive processes in the nerve, which follows the border between lateral and medial mesenchyme.

(C) The olfactory pit, dissected from an E10.5 embryo, viewed from above. The anterior pole is at the top (a), and the lateral nasal process is to the right (l). Pax-7 is limited to the lateral nasal process.

(D) Similar preparation to (C) showing the trajectory of the nascent olfactory nerve (black arrows), labeled with NCAM. All olfactory axons grow from the epithelium medially and then extend toward the anterior pole of the frontonasal mass.

(E) Coronal section through the frontonasal mass at E10.5 showing the relationship between NCAM-positive neurons and axons in the medial epithelium and mesenchyme (fluorescein label), and Pax-7-positive mesenchymal cells in the lateral mesenchyme (rhodamine label). White arrowheads indicate Pax-7 labeling in the lateral epithelium of the olfactory pit.

(F) Medial–lateral and anterior–posterior patterning occurs in vitro, based upon NCAM (blue) and Pax-7 (brown) labeling of epithelial cells, axons, and mesenchyme. The white and black arrows indicate the medial–lateral boundary in the epithelium.

eye) embryos (Hill et al., 1991) where RA is not produced by the frontonasal mesenchyme (Anchan et al., 1997). In *Pax-6*^{Sey}/*Pax-6*^{Sey} embryos that also carry one copy of the β*geo*6 transgene, β*geo*6 cells are specifically absent from the frontonasal mass (Figures 4E and 4F). Together, these results show that RA is a lateral signal whose availability depends upon the position of neural crest–associated cells in the frontonasal mass.

We then asked whether *FGF8*, *shh*, and *BMP4* define local signaling domains in the olfactory primordia. In the forebrain from E9.0 onward, *FGF8* and *shh* mRNA is restricted to a ventromedial domain (Figures 4G and 4H). There are few, if any, RA-producing mesenchymal cells immediately adjacent to this domain (Figure 4I). *FGF8*, *shh*, and *BMP4* cannot be detected in the surface epithelium at E9.0. However, as the olfactory placode begins to emerge, between E9.5 and E10.0, *FGF8* is seen in the medial epithelium of the frontonasal mass (Figure 4J and insert). At E10.5, after the olfactory epithelium has invaginated, *FGF8* is limited to a ridge of epithelium in the medial nasal process (Figure 4L). *shh* is not seen in the surface epithelium of the frontonasal mass at E9.5 (data not shown). By E10.5, however, *shh* is expressed in the medial nasal process in a band of cells at the posterior and medial margin (Figure 4M). Finally, from E9.5 onward, *BMP4* is expressed in the epithelium at the posterior boundary of the frontonasal mass and prepalatal region (Figure 4K). At E10.5, *BMP4* expression continues to define the posterior aspects of the medial and lateral nasal processes (Figure 4N). Thus, the expression patterns of *FGF8* and *shh* suggest that these molecules are associated with signaling from the medial forebrain and frontonasal mass, while *BMP4* is associated with the posterior aspect of the olfactory primordia.

RA Influences Lateral Differentiation

Based upon the local availability of RA, FGF8, shh, or the BMPs, it seemed likely that each of these signals might help establish medial–lateral and anterior–posterior distinctions in the developing olfactory pathway. To evaluate this possibility, we altered local signaling via RA (as well as FGF8, shh, or the BMPs; see below) either by blocking its function or expanding its range of action.

When the nonspecific alcohol dehydrogenase antagonist citral (which disrupts RA synthesis; Connor and Smit, 1987; Marsh-Armstrong et al., 1994; Anchan et al., 1997) is introduced in epithelial/mesenchymal cultures, differentiation is abolished and molecular markers are not seen in the remaining undifferentiated cell mass (data not shown). As an alternative to this extreme manipulation, we disrupted RA signaling using *Pax-6*^{Sey}/*Pax-6*^{Sey} embryos that lack RA-producing frontonasal mesenchymal cells. In these mutant embryos, there is no olfactory epithelium, and β-tubulin, NCAM, Pax-7, and RALDH-2 are not detected in the remaining surface epithelium or mesenchyme (Figure 5, top row, and data not shown). E9.0 wild-type epithelium recombined with mesenchyme from E9.0 *Pax-6*^{Sey} homozygotes (genotyped by PCR; data not shown) acquires some medial characteristics: β-tubulin and NCAM are expressed in cells scattered throughout the epithelium. Nevertheless, there is no clear medial–lateral axis, and Pax-7 is not seen (Figure 5, middle row). When *Pax-6*^{Sey} homozygous

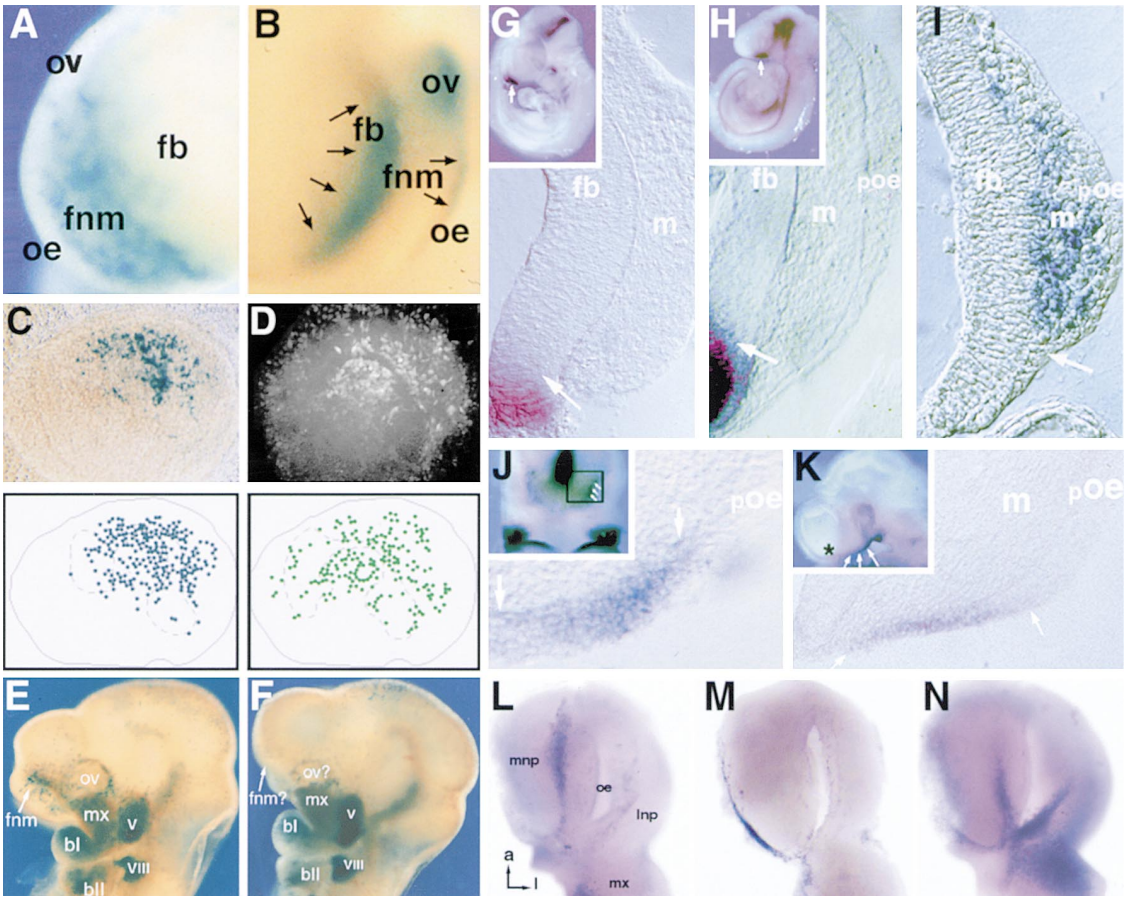

Figure 4. Inductive Signals Are Associated with Medial–Lateral and Anterior–Posterior Axes in the Developing Olfactory Pathway

(A) An E9.5–E10 β*geo*6 embryo shows that neural crest–associated cells are concentrated laterally (the position of the optic vesicle, ov, indicates the oblique view).

(B) Top/front view of an E9.5–E10 DR5-RARE indicator embryo shows domains of RA-mediated gene expression.

(C) An explant of an E10 frontonasal mass, cocultured on a monolayer of RA-indicator cells, shows the lateral concentration of β*geo*6-labeled cells (arrows).

(D) In vivo fluorescence image of RA-activated, GFP-expressing indicator cells beneath the mesenchymal surface of the explant in (C). Below (C) and (D) is a plot of β-gal- (blue) or GFP- (green) labeled cells showing registration of the two populations.

(E) β*geo*6 cells in the lateral frontonasal mesenchyme (arrow) and other cranial neural crest targets of a normal E10.5 embryo.

(F) A Pax6^{Sey}/Pax6^{Sey} littermate shows the specific absence of β*geo*6 cells from the frontonasal remnant (fnm?, arrow).

(G) A coronal section through an E9.0 embryo shows *FGF8* mRNA restricted to the ventromedial forebrain. The frontonasal mesenchyme is diminished in this region (arrow). The inset shows the distribution of FGF8 in the embryo from which this section was taken. The arrow indicates the location of the section.

(H) At E9.0, *shh* is seen in the ventromedial forebrain (arrow).

(I) Coronal section through an E9.0 embryo shows βgeo6-labeled mesenchyme adjacent to the presumptive olfactory epithelium and attenuated at the ventromedial forebrain (arrow).

(J) At E9.5, *FGF8* mRNA is found in the epithelium of the presumptive nasomedial process (inset black box, arrows) and excluded from the presumptive olfactory epithelium.

(K) *BMP4* is expressed in the presumptive palatal epithelium (between arrows), posterior to the presumptive olfactory epithelium. In the inset, the asterisk shows the approximate position of the presumptive olfactory epithelium.

(L) A dissected frontonasal process (oriented as indicated; anterior [a], lateral [l]) shows *FGF8* expression at E10.5 maintained in the epithelial ridge of the nasomedial process.

(M) At E10.5, *shh* is seen at the medial epithelial margin of the frontonasal process.

(N) At E10.5, *BMP4* is seen in the posterior epithelium of the lateral and medial nasal processes.

epithelium is recombined with normal mesenchyme, limited β-tubulin expression is seen in a thickened epithelial domain. NCAM is ectopically expressed in the mesenchyme, but Pax-7 expression is not detected (Figure 5, bottom row). Thus, the *Pax-6*^{Sey}-dependent loss of RA signaling from mesenchyme disrupts molecular differentiation associated with the lateral but not medial olfactory epithelium and mesenchyme. In contrast, *Pax-6*^{Sey} mutant epithelium does not respond to normal mesenchymal signals, nor can it maintain normal differentiation of frontonasal mesenchyme.

In the presence of excess RA (10^{-7} M), Pax-7 expression expands in an apparent medial direction (Figure 6, first row). To assess this change, we quantified Pax-7 expression in pairs of explants prepared from the same embryo; one side is treated, and the other is the control.

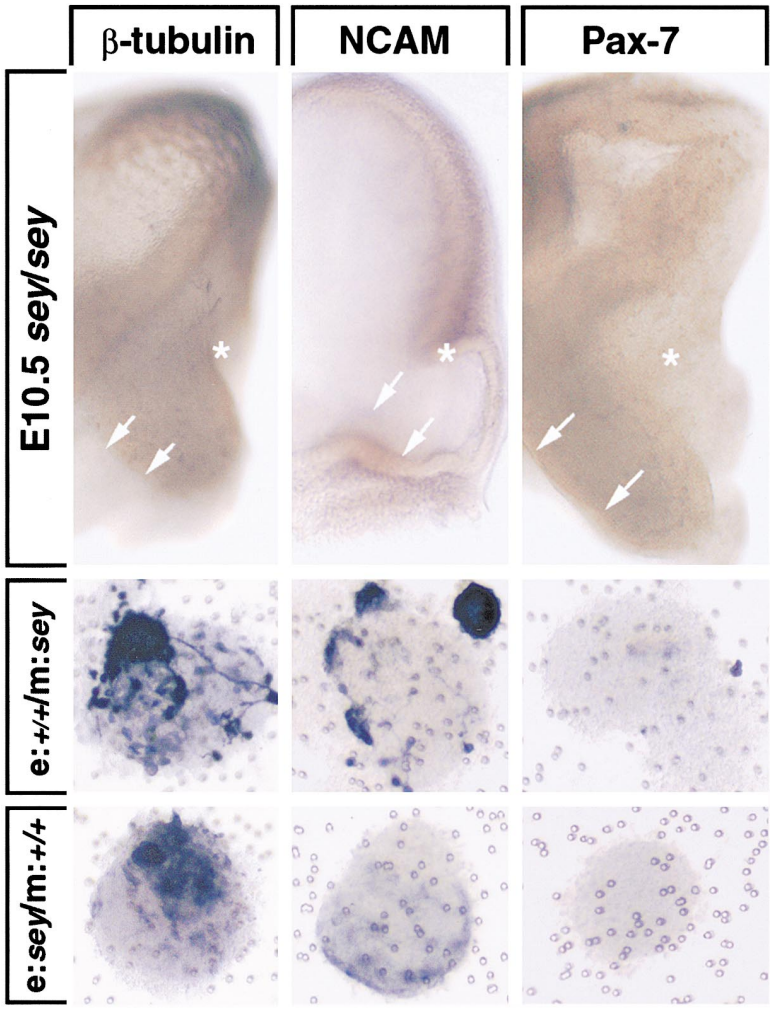

Figure 5. Medial Differentiation Persists while Lateral Differentiation Fails when RA-Producing Mesenchymal Cells Are Absent

First row: Front views of E10.5 Pax6^{Sey}/Pax6^{Sey} embryos. Arrows indicate approximate location of a remnant of the medionasal process; asterisks indicate region where lateral nasal process should be.

Second row: Recombination of normal epithelium with Pax6^{Sey}/Pax6^{Sey} mesenchyme results in expression of neuronal (medial) markers β-tubulin and NCAM but not the lateral mesenchymal marker Pax-7.

Third row: Recombination of Pax6^{Sey}/Pax6^{Sey} epithelium with normal mesenchyme does not fully restore molecular markers of axial or neuronal differentiation.

The percent difference of Pax-7 label between these pairs has been compared to pairs in which both sides remained untreated. In these pairs, an average of 57% more of the mesenchyme is labeled by Pax-7 in the RA-treated explant than in the untreated control explant as compared to untreated explant pairs ($p < 0.02$; Figure 7). There is no change in the overall size of the RA-treated explants versus their untreated control side; however, the relative size of the epithelium increases by ~30% in treated explants ($p < 0.0002$). The expansion of lateral mesenchyme and increase in proportion of epithelial area is accompanied by an apparent compression of NCAM-positive cells in the medial aspect of the epithelium. It is not possible to analyze this apparent change in the low magnification images shown in Figure 6. Accordingly, we assessed the numbers of NCAM-labeled cells throughout the entire depth of the olfactory epithelium using differential interference contrast optics at higher magnification so that individual labeled cells could be clearly resolved and counted in all focal planes (Figure 7). There is an average 30% reduction in the number of NCAM-positive cells compared to controls ($p < 0.006$; Figure 7). Thus, augmenting RA signaling enhances lateral differentiation of mesenchymal and epithelial components of the developing olfactory pathway and diminishes medial characteristics including neuronal differentiation.

FGF8b Influences Medial Differentiation

When FGF8b signaling is blocked using a function-blocking antibody (Dorkin et al., 1999), there is no significant change in explant size or epithelium size (Figure 6, second row). There is, however, an expansion of Pax-7 expression that approximates that seen in RA-treated explants (40% greater than control, $p < 0.03$; Figure 7). This is accompanied by a reduction in the number of NCAM-labeled neurons in the presumptive epithelium, also similar to that seen in RA-treated explants (Figure 7). In contrast, FGF8b protein (100 ng/ml) leads to a 57% increase in explant size and a corresponding increase in epithelial area (Figure 6, third row; $p < 0.0001$). In these explants, the area of Pax-7 expression is diminished by 45% ($p < 0.0002$; Figure 7). NCAM-labeled cells are seen throughout the epithelial domain, rather than restricted to the medial region (Figure 7), and NCAM-labeled neurites no longer form a coherent bundle at the lateral–medial interface (Figure 6). Finally, the number of NCAM-labeled cells, imaged and quantified throughout the

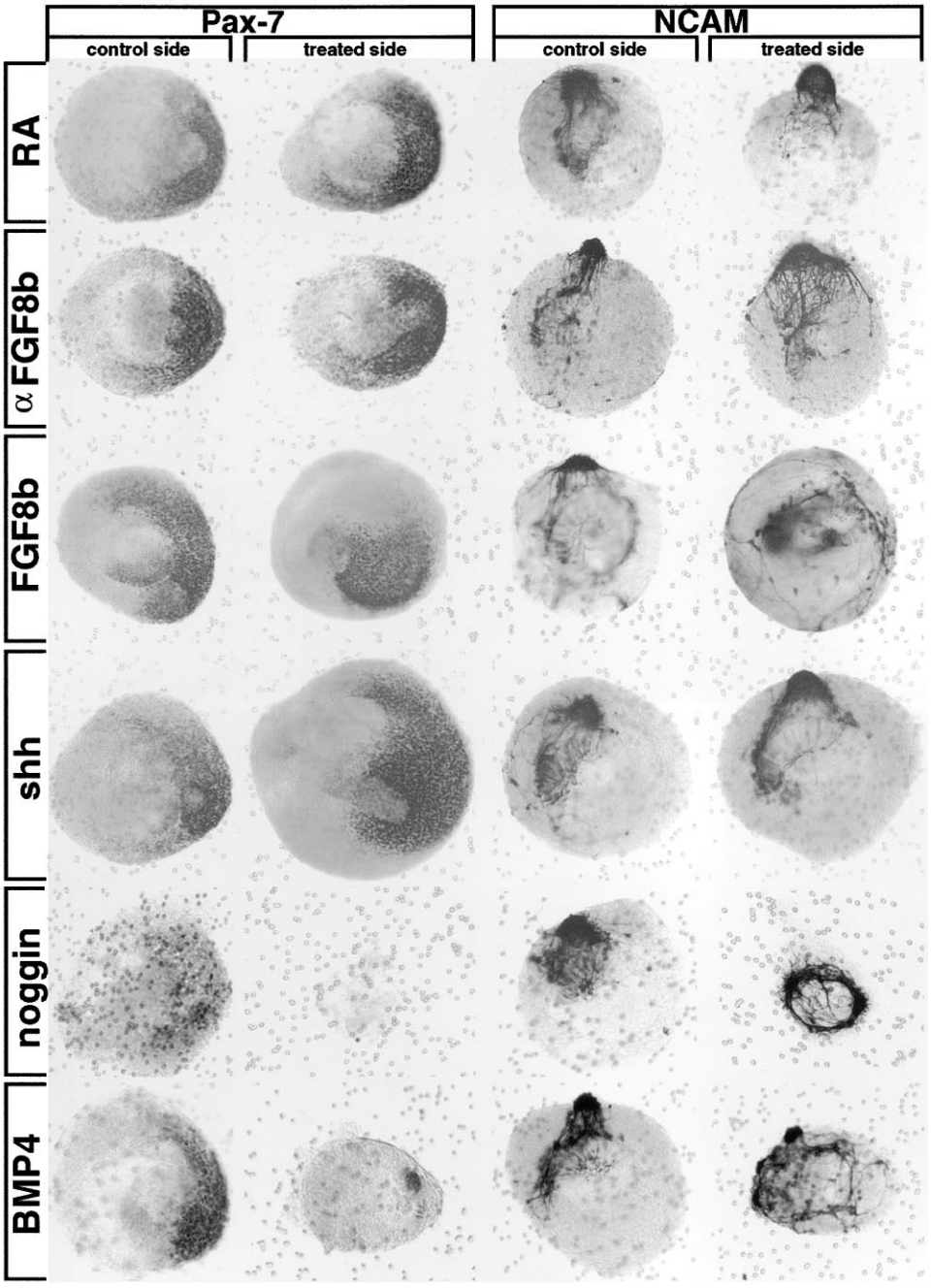

Figure 6. RA, FGF8b, shh, noggin, and BMP4 Influence Axes, Morphogenesis, and Cellular Differentiation of the Olfactory Epithelium and Nerve

At left: Pax-7 expression in explant pairs from the same embryo in which one side serves as an untreated control and the other has been exposed to RA, anti-FGF8b, recombinant FGF8b, shh, noggin, or BMP4 protein.
At right: NCAM expression in explant pairs.

thickness of the epithelium, is increased by an average of 85% (Figure 7). Thus, FGF8b enhances growth and neuronal differentiation in the frontonasal mass in conjunction with changes in medial epithelial and mesenchymal patterning as well as modifying the trajectory of the nascent olfactory nerve.

Shh Is a Growth Signal

Interfering with shh signaling using a function-blocking antibody (Ericson et al., 1997) has no measurable effect upon explant size, patterning, or cellular differentiation (data not shown). In contrast, explants exposed to exogenous shh protein (100 ng/ml) are 33% larger ($p < 0.002$). Despite this enhanced growth, there is no apparent shift of medial or lateral patterning (Figure 6, fourth row). Pax-7 is expressed in a proportionally similar area in shh-treated explants and controls, and there is no change in the overall number of NCAM-labeled cells (Figure 7). Furthermore, NCAM-labeled neurites are fasiculated and follow a normal anterior trajectory. These

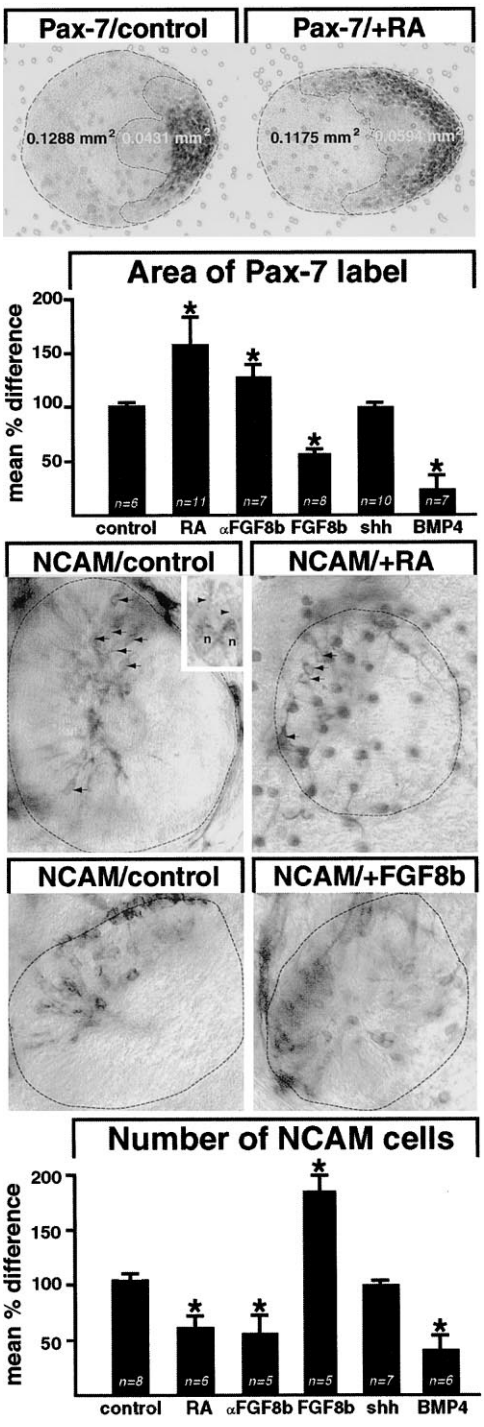

Figure 7. Quantitative Changes in Patterning and Cellular Differentiation in Response to Manipulating RA, FGF8b, shh, and BMP4 Signaling

Upper panel: A pair of explants showing the method for measuring Pax-7-labeled area (see Experimental Procedures for a complete explanation). The thick dotted line indicates the perimeter of the explant, which represents the total explant area (values in black), and the thin dotted line defines the perimeter of the Pax-7-labeled domain (values in white). The percentage of Pax-7 area for each explant was calculated by dividing the Pax-7 area by the total area. For the examples shown here, the control value is 35.7%, and the RA-treated value is 53.8%. Accordingly, the mean percentage difference for this explant pair is 151%.

results suggest that shh acts as a general growth signal in the olfactory primordia but does not seem to influence patterning of the olfactory epithelium and nerve.

BMPs Influence Anterior–Posterior and Neuronal Differentiation

When BMP signaling is inactivated in explant cultures by noggin (an endogenous BMP antagonist; Zimmerman et al., 1996), the entire frontonasal mesenchyme is lost and only a small epithelial region remains (Figure 6, fifth row; n = 21/21 pairs). In this remnant, Pax-7 is not detected (7/7 pairs); however, a patch of NCAM-positive cells is seen (12/12 pairs). Processes from these cells grow in a dense plexus around—but do not extend beyond—the perimeter of the explant. In contrast, BMP4 protein (20 ng/ml) decreases growth in frontonasal explants (Figure 6, sixth row) but leaves both mesenchymal and epithelial components. In the mesenchyme, there is a significant decrease in the area of Pax-7 expression (23%, $p < 0.004$; Figure 7), and the remaining Pax-7 domain is often shifted into the lateral epithelium. The number of NCAM-positive cells within the remaining epithelium decreases (an average of 38% of control values, $p < 0.003$; Figure 7) and a single, fasiculated olfactory nerve is no longer seen. There are, however, ectopic clusters of NCAM-expressing cells at the perimeter that extend processes throughout the explant. Thus, the BMPs provide posterior signals to influence the extent of mesenchymal and dermal differentiation and may influence neural differentiation in the olfactory epithelium via interaction with endogenous antagonists like noggin.

Discussion

Olfactory pathway development depends upon induction between frontonasal mesenchyme and adjacent ep-

Upper middle panel: A graph showing the mean percentage difference in Pax-7-labeled area for pairs of explants where inductive signals have been manipulated for one of the pairs. The control value represents explant pairs where both sides remained untreated. For each graph, n = number of pairs analyzed. Two-tailed t tests were performed, and asterisks indicate mean values that are significantly different from the control pairs ($p < 0.05$; individual values in text).

Middle panel: A pair of explants showing the method for identifying and counting NCAM-labeled cells in the presumptive olfactory epithelium and the effects of RA treatment. Each panel shows a single focal plane from the full through-focus series. Arrows indicate examples of cells that would be counted in each. Two representative cells that meet the criteria for counting (see Experimental Procedures) are shown in the inset at right. The nuclei are labeled (n), and the arrowheads indicate a process emerging from each cell. The total number of cells in this example (obtained from the complete through-focus series) is 47 for the control, and 19 for the RA-treated explant.

Lower middle panel: A pair of explants showing the effects of FGF8b treatment on the number and distribution of NCAM-labeled cells. NCAM-labeled cells are seen throughout the presumptive olfactory epithelium in the treated explant, rather than limited to the medial portion as in the control. The total number of cells in this example (obtained from the complete through-focus series) is 53 for the control and 77 for the FGF8b-treated explant.

Lower panel: A graph showing the percentage difference of NCAM-positive cells in the presumptive olfactory epithelium for the control versus treated side.

ithelia. As at other sites of mesenchymal/epithelial induction—especially the limbs, the branchial arches, and the aortic arches of the heart—the local actions of several signaling molecules contribute to distinct facets of this process. No single molecule, however, is uniquely responsible for morphogenesis and cellular differentiation in the olfactory pathway. Instead, when frontonasal mesenchymal/epithelial signaling is disrupted—by physical separation, by mutation, or by manipulation of signaling molecules—specific aspects of patterning and differentiation are compromised. The deficits reflect normal axial and cellular differentiation that accompanies mesenchymal/epithelial induction. Thus, the initial differentiation of the olfactory pathway relies upon a mechanism shared by the limbs, branchial arches, and heart that has been adapted for neural development in a functionally distinct forebrain pathway.

Induction and Olfactory Pathway Development

Mesenchymal/epithelial induction, in vitro, leads to a nearly complete spectrum of differentiated cells and structures in the embryonic olfactory epithelium and nerve (Cuschieri and Bannister, 1975; Miragall et al., 1989; Whitesides and LaMantia, 1996). Our results suggest that initial neural differentiation of the surface ectoderm to olfactory epithelium may rely upon BMP antagonists like noggin, perhaps in conjunction with FGF signals, as is the case for other neuralized regions of the ectoderm (Lamb and Harland, 1995; Bachiller et al., 2000). Furthermore, the initial differentiation of NCAM-positive neurons in the medial olfactory epithelium and the initial trajectory of their axons depends upon medial–lateral and anterior–posterior patterning in both the epithelium and mesenchyme. This may reflect the activity of FGF8b on the medial mesenchyme; however, it is unlikely that FGF8 acts directly on the epithelial cells to elicit neuronal differentiation (De Hamer et al., 1994). Finally, axon fasiculation and directed outgrowth of the olfactory nerve are similar to that in the embryo, where the forebrain is present (Whitesides and LaMantia, 1996). This implies that there is little target-derived guidance from the forebrain for the initial projection of the olfactory nerve. Instead, the initial growth of the olfactory nerve is influenced by the concerted action of signals like RA, FGF8, and the BMPs from the local sources within the frontonasal process.

Mesenchymal/epithelial induction may influence the initial formation of the olfactory bulb. The frontonasal mesenchyme is also apposed to the ventrolateral forebrain and at least one mesenchymal signal, RA, activates gene expression in the ventrolateral forebrain (LaMantia et al., 1993; Whitesides and LaMantia, 1996; Anchan et al., 1997). Furthermore, RA teratogenesis, *shh* inactivation, and the *Pax-6* mutation compromises the olfactory bulb as well as the epithelium and nerve (Chiang et al., 1996; Anchan et al., 1997; Dellovade et al., 1998). Finally, olfactory axons are not necessary for bulb morphogenesis in embryologically manipulated frogs or *Emx-2* mutant mice (Byrd and Burd, 1993; Yoshida et al., 1997). It is more likely that the axons influence later stages of bulb development (Stout and Graziadei, 1980; Gong and Shipley, 1995). Together, these observations suggest that mesenchymal/epithelial induction contributes to morphogenesis of the olfactory bulb.

Neural Crest and Mesenchymal/Epithelial Induction in the Olfactory Pathway

Neural crest–associated mesenchymal cells define a local source of RA in the lateral frontonasal mesenchyme, and olfactory pathway development is disrupted when this signal is absent. Recent analysis of cranial neural crest migration, cell death, and cell fate suggests a systematic relationship between neural crest–associated structures in the head and their origin or migration from specific locations in the hindbrain and midbrain (Serbedzija et al., 1992; Sechrist et al., 1993; Graham et al., 1994). The frontonasal mesenchymal cells described here probably originate from anterior mesencephalic levels of the neural tube and have a specific migratory path (Serbedzija et al., 1992; Osumi-Yamashita et al., 1994). Thus, the origin and migration of neural crest cells may help specify mesenchymal/epithelial induction in the olfactory pathway. There may be a similar relationship between origin and inductive capacity of neural crest in branchial arches (Lumsden, 1988; O'Connor and Tessier-Lavigne, 1999), aortic arches (Le Lievre and Le Dourain, 1975; Waldo et al., 1996; Creazzo et al., 1998), and limb buds (Shoobridge et al., 1983; Ros et al., 1997; Patapoutian et al., 1999). It is therefore possible that the origin of neural crest along the anterior–posterior axis helps to specify several sites of nonaxial mesenchymal/epithelial induction including the olfactory pathway.

Induction, the *Pax-6^{Sey}* Mutation, and Olfactory Pathway Development

Neither mesenchyme nor epithelium from *Pax-6^{Sey}* homozygous mutant embryos completely supports the development of an olfactory epithelium and nerve when recombined with their wild-type counterparts. Accordingly, prior to E9.0, Pax-6 must confer competence upon both tissues for inductive interactions that mediate olfactory pathway development. The loss of competence in homozygous mutant tissues might be due to the activity of mutant Pax-6 in the facial epithelium or dorsal forebrain (Grindley et al., 1995). Nevertheless, it also reflects the compromised state of the frontonasal mesenchyme, which lacks neural crest due to a deficit in the migratory pathway (Matsuo et al., 1993; Osumi-Yamashita et al., 1997) and which does not produce at least one signal, RA (Anchan et al., 1997). In the embryo and in recombined cultures with mutant mesenchyme or epithelium, lateral structures and expression of lateral markers in the olfactory pathway seem to be absent and corresponding medial differentiation is aberrant. Thus, the Pax-6 mutation compromises mesenchymal/epithelial signaling, including local RA signaling, that is essential for the initial differentiation of the olfactory epithelium and nerve.

Axes, Signals, and Olfactory Pathway Induction

At the best-studied site of mesenchymal/epithelial interaction—the limb bud (reviewed by Tickle and Eichele, 1994; Johnson and Tabin 1997)—the induction of axes based upon local signals is an essential first step in guiding subsequent morphogenesis and cellular differ-

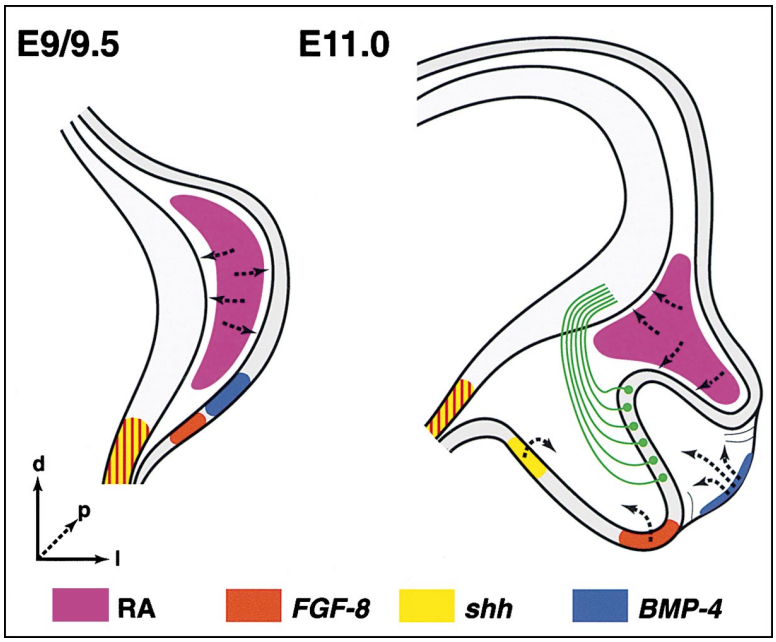

Figure 8. A Schematic of Axes and Signals that Influence Mesenchymal/Epithelial Induction in the Olfactory Pathway

Each drawing represents a section through the forebrain at the age indicated. The dorsal (d), posterior (p), and lateral (l) axes for each drawing are indicated at the bottom, left. The sources of four inductive signals commonly associated with mesenchymal/epithelial interactions are indicated diagrammatically, based upon the localization data in the text. The arrows associated with each local signaling source indicate our interpretation of the general direction in which these signals act in ongoing mesenchymal/epithelial interactions. These interpretations are based upon the results of the gain- and loss-of-function experiments that disrupt aspects of gene expression, morphogenesis, or cellular differentiation associated primarily with the lateral, medial, anterior, or posterior axes in the developing frontonasal mass.

entiation. Early embryological studies (Balinsky, 1933; reviewed by Slack, 1995) indicate that the olfactory primordia, when transplanted beneath flank ectoderm, can induce a limb. This observation raises the possibility that the frontonasal epithelium and mesenchyme shares significant inductive capacity with the limb; however, this possibility has never been explored. We have shown that mesenchymal/epithelial induction mediated by local molecular signals also found in the limb establishes axial coordinates for the developing olfactory pathway. Furthermore, these axes constrain neuronal differentiation in the olfactory epithelium and the trajectory of axons in the olfactory nerve. Thus, the cellular mechanisms and morphogenetic consequences of mesenchymal/epithelial induction in the olfactory pathway are analogous to those in the limb.

These axial constraints for olfactory pathway development provide a valuable framework for evaluating the contribution of several individual signals. RA, FGFs, shh, and BMPs have all been implicated in olfactory development (Shenefelt, 1972; LaMantia et al., 1993; De Hamer et al., 1994; Chiang et al., 1996; Lanoue et al., 1999; Shou et al., 1999). However, previous teratogenic, genetic, and pharmacological studies have not fully defined the endogenous contribution of each molecule to neuronal and nonneuronal differentiation. Our data shows that within the context of ongoing mesenchymal/epithelial interactions, each signal is associated with a single axis: RA is a lateral signal, FGF8 and shh are medial signals, and BMP4 is a posterior signal (Figure 8). The normal localization of each molecule supports these conclusions and the results of manipulating these signals are consistent with specific axial functions. When signaling via any one is disrupted, either by blocking or augmenting its function, there are consistent and predictable changes in morphogenesis, gene expression, and cellular differentiation. These changes focus upon a single axial direction with consequences for mesenchymal patterning, neuronal differentiation, or the growth of the olfactory nerve.

The four signals that we have examined do not by themselves account for olfactory pathway development, nor do they reflect the singular and direct effects of any of the four molecules on a specific cell type. Instead, they are common components of a molecular process for mesenchymal/epithelial interaction. In limbs, branchial arches, and heart, altering RA, shh, the FGFs, or the BMPs disrupts axis formation and corresponding morphogenesis (Helms et al., 1997; Johnson and Tabin, 1997; Neubüser et al., 1997; Barlow et al., 1999; Trumpp et al., 1999). At these sites, it is not possible to determine whether these signals act solely on mesenchyme or epithelium; nor can one assign any singular facet of cellular differentiation to a single signal. Similarly, it is not possible to assign the effects of RA, FGF8, shh, and BMP4 to any one cellular target in the olfactory pathway. Their concerted local action on subsets of mesenchymal and epithelial cells and subsequent additional signaling between these cells combine to elicit differentiation of olfactory neurons as well as the epithelial and skeletal elements in the frontonasal process.

We have analyzed the role of induction and inductive signals in the developing olfactory pathway primarily in an in vitro assay system. This approach permits greater physical access to the principle embryonic tissues that participate in induction and simplifies the manipulation of specific signals. Nevertheless, this system as well similar assays that have been used to examine mesenchymal/epithelial interactions in the mammalian branchial arches and limb buds (Neubüser et al., 1997; Weston et al., 2000) have some limitations. First, any distal signals, beyond the surface epithelium and adjacent mesenchyme, are eliminated from the sequence of interactions that lead to morphogenesis and development. Second, molecular manipulations done in vitro are often more effective in disrupting rather than aug-

menting developmental processes. Third, in vitro assays are limited in the epoch of development that can be examined. Accordingly, our in vitro results provide an outline of the cellular and molecular interactions that accompany a distinct period of early olfactory pathway morphogenesis. They do not, however, fully define the mechanisms that operate in vivo to direct specific cells and tissues to their final differentiated state in the intact olfactory system.

Induction, Peripheral Malformations, and Disrupted Forebrain Development

Limb, heart, face, and forebrain development can be disrupted by common teratogens, including RA as well as compounds or mutations that alter FGF, *shh*, or BMP signaling (Sulik and Sadler, 1993; Cooper et al., 1998; Meyers et al., 1998; Golden et al., 1999). Furthermore, clinical disorders that involve forebrain dysfunction are often correlated with limb, heart, and face malformations (reviewed by Waddington, 1993; LaMantia, 1999). Genetic studies of patients with these disorders have linked chromosomal deletions in loci that include inductive signals or patterning genes with vulnerability to a variety of behavioral and psychiatric diseases (reviewed by Driscoll and Emanuel, 1996; Goodman, 1998; LaMantia, 1999). Parallel studies of homologous genes in the mouse suggest that some genes from these loci may be preferentially expressed at sites of mesenchymal/epithelial induction, including the forebrain (Wilming et al., 1997; Lindsay et al., 1999; Yamagishi et al., 1999). We conclude that peripheral malformations and brain dysfunction in teratogenized or mutant individuals might reflect, in part, the disruption of a common inductive mechanism mediated by shared signals and related genes in the limbs, heart, face, and forebrain.

Experimental Procedures

Mice

Wild-type (CF-1, Charles River Labs; ICR, Harlan), transgenic, and mutant/transgenic embryos were obtained from timed pregnancies (morning after breeding = E0.5) generated in a breeding colony maintained by the Department of Laboratory Animal Medicine at University of North Carolina at Chapel Hill. Pregnant mice were killed by cervical dislocation and embryos harvested immediately. The β*geo*6 gene-trap line was generated by random insertion of a targeting vector in embryonic stem cells (Friedrich and Soriano, 1991). The presence of transgenes (in breeding males only) was confirmed by PCR of genomic DNA. *Pax6*^{Sey} homozygotes and littermates were PCR genotyped as described by Hill et al. (1991).

Histochemistry and Immunocytochemistry

β-gal histochemistry was performed using established protocols (LaMantia et al., 1993). For whole immunostained preparations, nickel chloride (0.05%) was used with diamino benzidine (DAB) to enhance detection of HRP-conjugated secondary antibodies. For double labeling, alkaline phosphatase was used with bromo chloro indole phosphate (BCIP) to give a blue reaction product, and HRP was used with DAB to give a brown reaction product. Specimens were labeled using rat monoclonal α-NCAM (Chemicon), mouse monoclonal α-β-tubulin (Babco), α-Pax-7 (SEI; Developmental Studies Hybridoma Bank), and a rabbit RALDH2 antiserum (P. McCaffery). These preparations were video imaged on a Leica photomacroscope. For double fluorescent labeling, 15 μm cryostat sections were incubated sequentially with rabbit α-β-gal (J. Sanes) followed by a mouse monoclonal α-nestin (RAT401; Developmental Studies Hybridoma Bank) or α-GAP43 (P. Skene); or rabbit polyclonal anti-NCAM (Chemicon) and mouse monoclonal α-Pax-7. Video images were obtained using a Leica epifluorescence microscope.

Explant Cocultures for RA Production

Cocultures of the E10 frontonasal mass (mesenchyme plus olfactory epithelium) and monolayers of RA-indicator cells were prepared as described previously (Colbert et al., 1993; LaMantia et al., 1993). A novel RA-sensitive cell line (the CE6 line) was clonally derived after transfecting mouse L cells with a DR5-RARE-thymidine kinase promoter driving a GFP reporter (GIBCO Green Lantern, GIBCO–BRL). The cell line was assessed for RA responses to 10^{-10} to 10^{-4} M *all-trans* RA. Cocultures of CE6 cell monolayers with frontonasal mesenchyme (and overlying epithelium) were imaged live using an inverted microscope. Images of GFP signal were collected, the orientation of the live explant was recorded by a brightfield image, and then the explants were prepared for β-gal histochemistry. β-gal-labeled preparations and matching GFP images were aligned by eye, using the image of the unfixed explant as a guide, and cells were plotted using video overlay software.

In Situ Hybridization

Antisense RNA probes for *shh*, *FGF8*, and *BMP4* were synthesized using plasmids containing either fragments or complete cDNAs (*shh* provided by A. McMahon; *FGF8* by G. Martin; *BMP4* by T. Michael Underhill). In situ hybridizations were performed using established protocols for whole embryos (Belo et al., 1997). Hybridized embryos were postfixed, embedded, and photographed, and then prepared for cryomicrotomy. Sections were imaged using differential interference contrast optics.

Mesenchyme/Epithelium Cocultures

The frontonasal mass including the forebrain neuroepithelium was dissected from E9.0 embryos. This trilaminar piece was transferred to 2.5% pancreatin/0.25% trypsin in L15 media for at least 30 min on ice (Neubüser et al., 1997). The tissue was then transferred to L15 media with 10% steroid-retinoid-depleted horse serum and each layer separated using sharpened tungsten microneedles. These pieces were cultured separately or recombined on 8 μm nucleopore filter circles floating on 3 ml DMEM/10% steroid-retinoid-stripped fetal bovine serum at 37°C in 95% room air/5% CO_2 for 48 hr. For manipulating signaling, *all-trans* RA (Sigma) was handled in yellow light and added to obtain a final concentration of 10^{-7} M. Recombinant mouse FGF8b and shh protein or recombinant human BMP4 protein (R&D Systems) was added at concentrations of 100 ng/ml (mFGF8b and mshh) or 20 ng/ml (hBMP4). Function blocking antibodies against FGF8b (R&D Systems) or shh (Developmental Studies Hybridoma Bank) were added at 1.0 μg/ml and 5.0 μg, respectively. CHO cells transfected with a *Xenopus* noggin expression construct as well as the parental CHO line (Lamb et al., 1993; kindly provided by Drs. R. Harland and J. M. DeJesus) were grown to ~50% confluence in 3 ml of αMEM in 35 mm dishes for 2 days. Freshly prepared explants were transferred directly to these dishes and cultured for another 48 hr. All cultures were imaged live and then fixed for immunohistochemistry.

Quantification of Area of Pax-7 Expression and Number of NCAM-Labeled Cells

Images were obtained of 49 Pax-7-labeled explant pairs from 98 individual embryos at an onscreen magnification of 16× with standard illumination on a Leica photomacroscope. Total area was measured by tracing the perimeter of each explant using NIH Image software. The Pax-7-labeled domain was defined as the area of contiguous Pax-7 immunoreactivity where cells with clearly labeled nuclei (where Pax-7 is expressed) are seen. In all explants there is an area of lighter Pax-7 immunoreactivity in the presumptive olfactory epithelium. This region was included in the area measurements; however, the percentage differences between control and experimental sides do not change if only mesenchymal Pax-7 is measured. The percentage of Pax-7-labeled area was calculated by dividing the Pax-7-labeled area by the total explant area. These values were compared only within sets of explants from individual embryos. For each treatment, the mean percentage difference of the explant pairs

was calculated and then compared with that of pairs where neither side was exposed to inductive signals or antagonists.

To count NCAM-labeled cells, 37 pairs of explants from 64 individual embryos were imaged using differential interference contrast optics at an onscreen magnfication of 230× with a Hammatsu ORCA video camera on a Leica DMR microscope. The outline of the epithelium was determined, and the depth of the initial focal plane where NCAM-labeled cells could be seen was established using a z axis micrometer. NCAM-labeled cells were identified based upon the following criteria: each cell has a visible nucleus surrounded by NCAM-labeled cytoplasm and an apical or basal extension. Such cells were counted by overlaying a counting mark in a separate video layer; then the objective was advanced to a focal plane 10 μm deeper. By focusing back to the previous layer, previously counted cells were excluded and labeled cells in the relevant focal plane were counted. This was repeated until an entire through-focus series was obtained and all cells were counted. For each explant pair, the percentage difference was calculated by dividing the number of NCAM-labeled cells in the treated explant by that in the untreated control. The mean percentage difference was then calculated for each individual treatment group and compared statistically with that from pairs of untreated explants.

Acknowledgments

It is a particular pleasure to dedicate this paper to Dr. Viktor Hamburger on the occasion of his 100th birthday in honor of his inspiration to several generations of developmental neurobiologists, including the first author of this paper. We thank Tom Maynard for thoughtful criticism and assistance with figures. Patricia Maness, Jean Lauder, Bill Snider, Eva Anton, Gail Burd, and the anonymous reviewers all provided helpful comments on the manuscript. R. Anchan, M. B. Thomas, and L. Lewis-Tuffin contributed to early phases of this work. C. Haines, S. Mann, and C. Gurtler provided technical assistance at various points. The β-*geo*6 mice were made in the laboratory of Dr. Jane Dodd, using a targeting vector provided by Dr. Phillipe Soriano. This work was supported by HD29178, the Wodecroft Foundation via the National Alliance for Schizophrenia and Affective Disorders (NARSAD), and a Howard Hughes Pilot Grant for the Study of Animal Models for Neurological Disease to the University of North Carolina at Chapel Hill School of Medicine.

Received March 1, 2000; revised September 28, 2000.

References

Anchan, R.M., Drake, D.P., Gerwe, E.A., Haines, C.F., and LaMantia, A.-S. (1997). A failure of retinoid-mediated induction accompanies the loss of the olfactory pathway during mammalian forebrain development. J. Comp. Neurol. *379*, 171–184.

Balinsky, B.I. (1933). Das extremitätenseiten feld, seine ausdehnung und beschaffenheit. Wilhelm Roux Arch. Entw Mech. Org. *130*, 704–746.

Barlow, A.J., Bogardi, J.P., Ladher, R., and Francis-West, P.H. (1999). Expression of chick Barx-1 and its differential regulation by FGF-8 and BMP signaling in the maxillary primordia. Dev. Dynam. *214*, 291–302.

Bachiller, D., Klingensmith, J., Kemp, C., Belo, J.A., Anderson, R.M., May, S.R., McMahon, J.A., McMahon, A.P., Harland, R.M., Rossant, J., and De Robertis, E.M. (2000). The organizer factors Chordin and Noggin are required for mouse forebrain development. Nature *403*, 658–661.

Belo, J.A., Bouwmeester, T., Leyns, L., Kertesz, N., Gallo, M., Follettie, M., and DeRobertis, E.M. (1997). Cerberus-like is a secreted factor with neuraliziing activity expressed in the anterior primeitev endoderm of the mouse gastrula. Mech. Dev. *68*, 45–57.

Benowitz, L.I., Apostolides, P.J., Perrone-Bizzozero, N., Finkelstein, S.P., and Zwiers, H. (1988). Anatomical distribution of the growth associated protein GAP-43/B-50 in the adult rat brain. J. Neurosci. *8*, 339–352.

Byrd, C.A., and Burd, G.D. (1993). Morphological and quantitative evaluation of olfactory bulb development in Xenopus after olfactory placode transplantation. J. Comp. Neurol. *331*, 551–563.

Calof, A.L., and Chikaraishi, D.M. (1989). Analysis of neurogenesis in a mammalian neuroepithelium: proliferation and differentiation of an olfactory neuron precursor in vitro. Neuron *3*, 115–127.

Chiang, C., Litingtung, Y., Lee, E., Young, K.E., Corden, J.L., Westphal, H., and Beachy, P.A. (1996). Cyclopia and defective axial patterning in mice lacking Sonic hedgehog gene function. Nature *383*, 407–413.

Colbert, M.C., Linney, E., and LaMantia, A.-S. (1993). Local sources of retinoic acid coincide with retinoid-mediated transgene activity during embryonic development. Proc. Natl. Acad. Sci. USA *90*, 6572–6576.

Connor, M., and Smit, M.H. (1987). Terminal-group oxidation of retinol by mouse epidermis: inhibition in vitro and in vivo. Biochem. J. *244*, 489–492.

Cooper, M.K., Porter, J.A., Young, K.E., and Beachy, P.A. (1998). Teratogen-mediated inhibition of target tissue response to *Shh* signaling. Science *280*, 1603–1607.

Creazzo, T.L., Godt, R.E., Leatherbury, L., Conway, S.J., and Kirby, M.L. (1998). Role of cardiac neural crest cells in cardiovascular development. Annu. Rev. Physiol. *60*, 267–286.

Crossley, P.H., and Martin, G.R. (1995). The mouse *Fgf8* gene encodes a family of polypeptides and is expressed in regions that direct outgrowth and patterning in the developing embryo. Development *121*, 439–451.

Croucher, S.J., and Tickle, C. (1989). Characterization of epithelial domains in the nasal passages of chick embryos: spatial and temporal mapping of a range of extracellular matrix and cell surface molecules during development of the nasal placode. Development *106*, 493–509.

Cuschieri, A., and Bannister, L.H. (1975). The development of the olfactory mucosa in the mouse: light microscopy. J. Anat. *119*, 277–286.

DeHamer, M.K., Guevara, J.L., Hannon, K., Olwin, B.B., and Calof, A.L. (1994). Genesis of olfactory receptor neurons in vitro: regulation of progenitor cell divisions by fibroblast growth factors. Neuron *13*, 1083–1097.

Dellovade, T.L., Pfaff, D.W., and Schwanzel-Fukuda, M. (1998). Olfactory bulb development is altered in small-eye (Sey) mice. J. Comp. Neurol. *402*, 402–418.

Dorkin, T.J., Robinson, M.C., Marsh, C., Bjartell, A., Neal, D.E., and Leung, H.Y. (1999). FGF8 over-expression in prostate cancer is associated with decreased patient survival and persists in androgen independent disease. Oncogene *18*, 2755–2761.

Doucette, R. (1990). Glial influences on axonal growth in the primary olfactory system. Glia *3*, 433–449.

Driscoll, D.A., and Emanuel, B.S. (1996). DiGeorge and Velocardiofacial Syndromes: the 22q11 deletion syndrome. Ment. Retard. Dev. Disabil. Res. Rev. *2*, 130–138.

Easter, S.S., Jr., Ross, L.S., and Frankfurter, A. (1993). Initial tract formation in the mouse brain. J. Neurosci. *13*, 285–299.

Echelard, Y., Epstein, D.J., St-Jacques, B., Shen, L., Mohler, J., McMahon, J.A., and McMahon, A.P. (1993). Sonic hedgehog, a member of a family of putative signaling molecules, is implicated in the regulation of CNS polarity. Cell *75*, 1417–1430.

Ericson, J., Rashbass, P., Schedl, A., Brenner-Morton, S., Kawakami, A., van Heyningen, V., Jessell, T.M., and Briscoe, J. (1997). Pax6 controls progenitor cell identity and neuronal fate in response to graded Shh signaling. Cell *90*, 169–180.

Farbman, A.I. (1988). Cellular interactions in the development of the vertebrate olfactory system. In Molecular Neurobiology of the Olfactory System, F.L. Margolis and T.V. Getchell, eds. (New York: Plenum Press), pp. 319–332.

Farbman, A.I. (1992). Cell Biology of Olfaction (Cambridge: Cambridge University Press), pp.167–206.

Francis-West, P.H., Tatla, T., and Brickell, P.M. (1994). Expression patterns of the bone morphogenetic protein genes Bmp-4 and

Bmp-2 in the developing chick face suggest a role in outgrowth of the primordia. Dev. Dyn. *201*, 168–178.

Francis-West, P., Ladher, R., Barlow, A., and Graveson, A. (1998). Signaling interactions during facial development. Mech. Dev. *75*, 3–28.

Friedrich, G., and Soriano, P. (1991). Promoter traps in embryonic stem cells: a genetic screen to identify and mutate developmental genes in mice. Genes Dev. *5*, 1513–1523.

Golden, J.A., Bracilovic, A., McFadden, K.A., Beesley, J.S., Rubenstein, J.L., and Grinspan, J.B. (1999). Ectopic bone morphogenetic proteins 5 and 4 in the chicken forebrain lead to cyclopia and holoprosencephaly. Proc. Natl. Acad. Sci. USA *96*, 2439–2444.

Gong, Q., and Shipley, M.T. (1995). Evidence that pioneer olfactory axons regulate telencephalon cell cycle kinetics to induce the formation of the olfactory bulb. Neuron *14*, 91–101.

Goodman, A.B. (1998). Three independent lines of evidence suggest retinoids as causal to schizophrenia. Proc. Natl. Acad. Sci USA *95*, 7240–7244.

Graham, A., Francis-West, P., Brickell, P., and Lumsden, A. (1994). The signaling molecule BMP4 mediates apoptosis in the rhombencephalic neural crest. Nature *372*, 684–686.

Grindley, J.C., Davidson, D.R., and Hill, R.E. (1995). The role of *Pax-6* in eye and nasal development. Development *121*, 1433–1442.

Heikinheimo, M., Lawshe, A., Shackleford, G.M., Wilson, D.B., and MacArthur, C.A. (1994). *Fgf-8* expression in the post-gastrulation mouse suggests roles in the development of the face, limbs, and central nervous system. Mech. Dev. *48*, 129–138.

Helms, J.A., Kim, C.H., Hu, D., Minkoff, R., Thaller, C., and Eichele, G. (1997). Sonic hedgehog participates in craniofacial morphogenesis and is down-regulated by teratogenic doses of retinoic acid. Dev. Biol. *187*, 25–35.

Hill, R.E., Favor, J., Hogan, B.L.M., Ton, C.C.T., Saunders, G.F., Hanson, I.M., Prosser, J., Jordan, T., Hastie, N.D., and van Heyningen, V. (1991). Mouse *small eye* results from mutations in a paired-like homeobox-containing gene. Nature *354*, 522–525.

Hinds, J.W. (1968). Autoradiographic study of histogenesis in the mouse olfactory bulb. II. Cell proliferation and migration. J. Comp. Neurol. *134*, 305–322.

Jacobson, A.G. (1963). The determination and positioning of the nose, lens and ear. I. Interactions within the ectoderm and between the ectoderm and underlying tissues. J. Exp. Zool. *154*, 273–284.

Johnson, R.L., and Tabin, C.J. (1997). Molecular models for vertebrate limb development. Cell *90*, 979–990.

Key, B., and Akeson, R.A. (1990). Olfactory neurons express a unique glycosylated form of the neural cell adhesion molecule NCAM. J. Cell Biol. *110*, 1729–1743.

Lamb, T.M., and Harland, R.M. (1995). Fibroblast growth factor is a direct neural inducer, which combined with noggin generates anterior-posterior neural pattern. Development *121*, 3627–3636.

Lamb, T.M., Knecht, A.K., Smith, W.C., Stachel, S.E., Economides, A.N., Stahl, N., Yancopolous, G.D., and Harland, R.M. (1993). Neural induction by the secreted polypeptide noggin. Science *262*, 713–718.

LaMantia, A.-S. (1999). Forebrain induction, retinoic acid, and vulnerability to schizophrenia: insights from molecular and genetic analysis in developing mice. Biol. Psychiatry *46*, 19–30.

LaMantia, A.-S., Colbert, M.C., and Linney, E. (1993). Retinoic acid induction and regional differentiation prefigure olfactory pathway formation in the mammalian forebrain. Neuron *10*, 1035–1048.

Lanoue, L., Dehart, D.B., Hinsdale, M.E., Maeda, N., Tint, G.S., and Sulik, K.K. (1999). Limb, genital, CNS, and facial malformations result from gene/environment-induced cholesterol deficiency: further evidence for a link to sonic hedgehog. Am. J. Med. Genet. *73*, 24–31.

Laufer, E., Nelson, C.E., Johnson, R.L., Morgan, B.A., and Tabin, C. (1994). Sonic hedgehog and Fgf-4 act through a signaling cascade and feedback loop to integrate growth and patterning of the developing limb bud. Cell *79*, 993–1003.

Le Leivre, C.S., and Le Dourain, N.M. (1975). Mesenchymal derivatives of the neural crest: analysis of chimareic quail and chick embryos. J. Embryol. Exp. Morph. *34*, 125–154.

Lindsay, E.A., Botta, A., Jurecic, V., Carattini-Rivera, S., Cheah, Y.C., Rosenblatt, H.M., Bradley, A., and Baldini, A. (1999). Congenital heart disease in mice deficient for the DiGeorge syndrome region. Nature *401*, 379–383.

Lumsden, A.G.S. (1988). Spatial organization of the epithelium and the role of neural crest cells in the initiation of the mammalian tooth germ. Development *103*, 155–169.

Lumsden, A., and Krumlauf, R. (1996). Patterning the vertebrate neuraxis. Science *274*, 1109–1115.

Mansouri, A., Stoykova, A., Torres, M., and Gruss, P. (1996). Dysgenesis of cephalic neural crest derivatives in Pax7−/− mutant mice. Development *122*, 831–838.

Marsh-Armstrong, N., McCaffery, P., Gilbert, W., Dowling, J.E., and Drager, U.C. (1994). Retinoic acid is necessary for the development of the ventral retina in zebrafish. Proc. Natl. Acad. Sci. USA *91*, 7286–7290.

Matsuo, T., Osumi-Yamashita, N., Noji, S., Ohuchi, H., Koyama, E., Myokai, N., Matsuo, F., Taniguchi, S., Doi, H., Iseki, S., et al. (1993). A mutation in the *Pax6* gene in rat *small eye* is associated with impaired migration of midbrain crest cells. Nat. Genet. *3*, 299–304.

Meyers, E.N., Lewandoski, M., and Martin, G.R. (1998). An Fgf8 mutant allelic series generated by Cre- and Flp-mediated recombination. Nat. Genet. *18*, 136–141.

Miragall, F., Kadmon, M., Husmann, M., and Schachner, M. (1989). Expression of L1 and NCAM cell adhesion molecules during development of the mouse olfactory system. Dev. Biol. *135*, 272–286.

Niederrethier, K., Subbarayan, V., Dolle, P., and Chambon, C. (1999). Embryonic retinoic acid synthesis is essential for early mouse postimplantation development. Nat. Genet. *21*, 444–448.

Neubüser, A., Peters, H., Balling, R., and Martin, G.R. (1997). Antagonistic interactions between FGF and BMP signaling pathways: a mechanism for positioning the sites of tooth formation. Cell *90*, 247–255.

O'Connor, R., and Tessier-Lavigne, M. (1999). Identification of maxillary factor, a maxillary process-derived chemoattractant for developing trigeminal sensory axons. Neuron *24*, 165–178.

Osumi-Yamashita, N., Ninomiya, Y., Doi, H., and Eto, K. (1994). The contribution of both forebrain and midbrain crest cells to the mesenchyme in the frontonasal mass of mouse embryos. Dev. Biol. *164*, 409–419.

Osumi-Yamashita, N., Kuratani, S., Ninomiya, Y., Aoki, K., Iseki, S., Chareonvit, S., Doi, H., Fujiwara, M., Watanabe, T., and Eto, K. (1997). Cranial anomaly of homozygous *rSey* rat is associated with a defect in the migration pathway of midbrain crest cells. Dev. Growth Differ. *39*, 53–67.

Patapoutian, A., Backus, C., Kispert, A., and Reichardt, L.F. (1999). Regulation of neurotrophin-3 expression by epithelial-mesenchymal interactions: the role of Wnt factors. Science *283*, 1180–1183.

Richman, J.M., and Tickle, C. (1989). Epithelia are interchangeable between facial primordia of chick embryos and morphogenesis is controlled by the mesenchyme. Dev. Biol. *136*, 201–210.

Rollhauser-ter Horst, R.J. (1975). Neural crest and early forelimb development in amphibia. Anat. Embryol. *147*, 337–344.

Ros, M.A., Sefton, M., and Nieto, M.A. (1997). Slug, a zinc finger gene previously implicated in the early patterning of the mesoderm and the neural crest, is also involved in chick limb development. Development *124*, 1821–1829.

Roskams, A.J., Cai, X., and Ronnett, G.V. (1998). Expression of neuron-specific beta-III tubulin during olfactory neurogenesis in the embryonic and adult rat. Neuroscience *83*, 191–200.

Rubenstein, J.L., and Beachy, P.A. (1998). Patterning of the embryonic forebrain. Curr. Opin. Neurobiol. *8*, 18–26.

Schwanzel-Fukuda, M., Abraham, S., Crossin, K.L., Edelman, G.M., and Pfaff, D.W. (1992). Immunocytochemical demonstration of neural cell adhesion molecule (NCAM) along the migration route of luteinizing hormone-releasing hormone (LHRH) neurons in mice. J. Comp. Neurol. *321*, 1–18.

Sechrist, J., Serbedzija, G.N., Scherson, T., Fraser, S.E., and Bronner-Fraser, M. (1993). Segmental migration of the hindbrain neural crest does not arise from its segmental generation. Development *118*, 691–703.

Serbedzija, G.N., Bronner-Fraser, M., and Fraser, S.E. (1992). Vital dye analysis of cranial neural crest cell migration in the mouse embryo. Development *116*, 297–307.

Shenefelt, R.E. (1972). Morphogenesis of malformations in hamsters caused by retinoic acid: relations to dose and stage at treatment. Teratology *5*, 104–118.

Shoobridge, R., Velkou, D., and McCredie, J. (1983). Neural crest ablation and limb morphogenesis. J. Exp. Zool. *225*, 73–87.

Shou, J., Rim, P.C., and Calof, A.L. (1999). BMPs inhibit neurogenesis by a mechanism involving degradation of a transcription factor. Nat. Neurosci. *2*, 339–345.

Slack, J.M.W. (1995). Growth factor lends a hand. Nature *374*, 217–218.

Sockanathan, S., and Jessell, T.M. (1998). Motor neuron-derived retinoid signaling specifies the subtype identity of spinal motor neurons. Cell *94*, 503–514.

Stemple, D.L., and Anderson, D.J. (1992). Isolation of a stem cell for neurons and glia from the mammalian neural crest. Cell *71*, 973–975.

Stout, R.P., and Graziadei, P.P.C. (1980). Influence of the olfactory placode on the development of the brain in *Xenopus Laevis* (Daudin). I. Axonal growth and connections of the transplanted olfactory placode. Neuroscience *5*, 2175–2186.

Sulik, K.K., and Sadler, T.W. (1993). Postulated mechanisms underlying the development of neural tube defects. Insights from in vitro and in vivo studies. Ann. NY Acad. Sci. *678*, 8–21.

Tanabe, Y., and Jessell, T.M. (1996). Diversity and pattern in the developing spinal cord. Science *274*, 1115–1123.

Tickle, C., and Eichele, G. (1994). Vertebrate limb development. Annu. Rev. Cell Biol. *10*, 121–152.

Trumpp, A., Depew, M.J., Rubenstein, J.L., Bishop, J.M., and Martin, G.R. (1999). Cre-mediated gene inactivation demonstrates that FGF8 is required for cell survival and patterning of the first branchial arch. Genes Dev. *13*, 3136–3148.

Vogel, A., Rodriguez, C., and Izpisua-Belmonte, J.C. (1996). Involvement of FGF-8 in initiation, outgrowth and patterning of the vertebrate limb. Development *122*, 1737–1750.

Waddington, J.L. (1993). Schizophrenia: developmental neuroscience and pathobiology. Lancet *341*, 531–536.

Waldo, K.L., Kuminski, D., and Kirby, M.L. (1996). Cardiac neural crest is essential for the persistence rather that than the formation of an arch artery. Dev. Dynam. *205*, 281–292.

Weston, A.D., Rosen, V., Chandraratna, R.A., and Underhill, T.M. (2000). Regulation of skeletal progenitor differentiation by the BMP and retinoid signaling pathways. J. Cell Biol. *148*, 679–690.

Whitesides, J.G., and LaMantia, A.-S. (1996). Differential adhesion and the initial assembly of the mammalian olfactory nerve. J. Comp. Neurol. *373*, 240–254.

Wilming, L.G., Snoeren, C.A.S., van Rijswijk, A., Grosveld, F., and Meijers, C.J. (1997). The murine homologue of HIRA, a DiGeorge syndrome candidate gene, is expressed in embryonic structures affected in human CATCH22 patients. Hum. Mol. Genet. *6*, 247–258.

Wray, S., Grant, P., and Gainer, H. (1989). Evidence that cells expressing luteinizing hormone-releasing hormone mRNA in the mouse are derived from progenitor cells in the olfactory placode. Proc. Natl. Acad. Sci. USA *86*, 8132–8136.

Yamagishi, H., Garg, V., Matsuoka, R., Thomas, T., and Srvivastava, D. (1999). A molecular pathway revealing a genetic basis for human cardiac and craniofacial defects. Science *283*, 1158–1161.

Yoshida, M., Suda, Y., Matsuo, I., Miyamoto, N., Takeda, N., Kuatani, S., and Aizawa, S. (1997). *Emx1* and *Emx2* functions in development of dorsal telencephalon. Development *124*, 101–111.

Zambrowicz, B.P., Imamoto, A., Fiering, S., Herzenberg, L.A., Kerr, W.G., and Soriano, P. (1997). Disruption of overlapping transcripts in the ROSA βgeo 26 gene trap strain leads to widespread expression of beta-galactosidase in mouse embryos and hematopoietic cells. Proc. Nat. Acad. Sci USA *94*, 3789–3794.

Zhao, D., McCaffery, P., Ivins, K.J., Neve, R.L., Hogan, P., Chin, W.W., and Drager, U.C. (1996). Molecular identification of a major retinoic-acid-synthesizing enzyme, aretinaldehyde-specific dehydrogenase. Eur. J. Biochem. *240*, 15–22.

Zimmerman, L.B., De Jesus-Escobar, J.M., and Harland, R.M. (1996). The Spemann organizer signal noggin binds and inactivates bone morphogenetic protein 4. Cell *86*, 599–606.